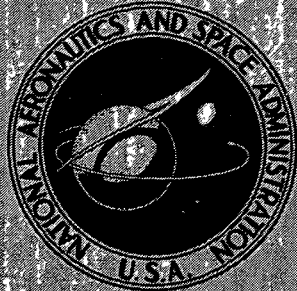


N73-12292

NASA CONTRACTOR
REPORT



NASA CR-2172

NASA CR-2172

CASE FILE
COPY

MASS DIFFUSION IN
A SELF-CONFINED ROTATING FLOW

by K. E. Torrance

Prepared by

CORNELL UNIVERSITY

Ithaca, N.Y. 14850

for Lewis Research Center

NATIONAL AERONAUTICS AND SPACE ADMINISTRATION • WASHINGTON, D. C. • NOVEMBER 1972

1. Report No. NASA CR-2172	2. Government Accession No.	3. Recipient's Catalog No.	
4. Title and Subtitle MASS DIFFUSION IN A SELF-CONFINED ROTATING FLOW		5. Report Date November 1972	
		6. Performing Organization Code	
7. Author(s) K. E. Torrance		8. Performing Organization Report No. None	
9. Performing Organization Name and Address Cornell University Ithaca, New York 14850		10. Work Unit No.	
		11. Contract or Grant No. NGL 33-010-042	
12. Sponsoring Agency Name and Address National Aeronautics and Space Administration Washington, D.C. 20546		13. Type of Report and Period Covered Contractor Report	
		14. Sponsoring Agency Code	
15. Supplementary Notes Project Manager, John C. Evvard, NASA Lewis Research Center, Cleveland, Ohio			
16. Abstract The effectiveness of fluid containment near an interior stagnation point and within a self-confined stagnation region is determined by numerically solving the species conservation equation for a bi-component mixture. The flow geometry is that of a swirling fluid stream containing a stationary eddy on the axis of rotation. The base flow is axisymmetric, and the Reynolds number is equal to 50. Schmidt numbers range from 0.1 to 10.			
17. Key Words (Suggested by Author(s)) Fluid confinement Mass diffusion Vortex flows		18. Distribution Statement Unclassified - unlimited	
19. Security Classif. (of this report) Unclassified	20. Security Classif. (of this page) Unclassified	21. No. of Pages 12	22. Price* \$3.00

* For sale by the National Technical Information Service, Springfield, Virginia 22151

SUMMARY

The effectiveness of fluid containment near an interior stagnation point and within a self-confined stagnation region is determined by numerically solving the species conservation equation for a bi-component mixture. The flow geometry is that of a swirling fluid stream containing a stationary eddy on the axis of rotation. The base flow is axisymmetric and the Reynolds number is equal to 50. Schmidt numbers range from 0.1 to 10.

INTRODUCTION

Containment of one fluid by a suitably-directed stream (or streams) of another fluid is a problem of considerable practical interest, particularly for the generation of power from chemical and nuclear fuels. Several containment schemes have been suggested which focus on the establishment of some sort of closed recirculation zone [1,2]. Mass exchange by diffusion eventually depletes any fluid initially contained in the zone, however, and replenishment of critical species is required. The present report examines diffusional loss from a particular containment zone and the feasibility of using a small supply stream to replenish critical species to the zone. These will be referred to as Problem I - Depletion and Problem II - Filling, respectively.

FLOW FIELD

The containment geometry considered is that of an axisymmetric eddy situated on the axis of rotation of a swirling, translating fluid stream. The initiation and structure of such eddies has been reported previously [3]. That study provides additional details and is used as a basis for the work presented here. Axisymmetric, incompressible flow through a cylindrical streamtube is considered with axial and radial co-ordinates denoted by x and r . Appropriate scaling parameters are the tube radius, r_0 , the mean through-flow velocity in the tube, U , and the angular velocity of the tube wall, ω_0 . Fluid enters the tube at $x = 0$ with axial, radial, and azimuthal velocity components given by $u = 1$, $v = 0$, and $w = r^{-1} [1 - \exp(-Br^2)]$. All variables are dimensionless and B is a constant in the exponential vortex velocity profile. The tube wall is impermeable, frictionless, and five radius units in length. The partial differential equations governing the flow field were solved by a finite difference scheme in reference [3]: The governing parameters appear as a Reynolds number, $Re = Ur_0/v$, and a swirl ratio, $\Gamma = r_0\omega_0/U$, where v is the kinematic viscosity. Note that Re is based on tube radius.

Streamlines for a flow with a vortex breakdown eddy present are shown in Fig. 3(a) for the case $Re = 50$, $\Gamma = 1$ and $B = 8$. The cited flow is the flow field used for study in the present report. The external stream flows from left to right over the eddy (which is stationary in space) forming two stagnation points along the axis. The boundary of the eddy is denoted by $\psi = 0$. The dotted line in Fig. 3(a) is the finite difference representation of the boundary. Since there is no net mass flow across a streamline, the eddy

represents a fluid region totally confined by the external stream. As Re or Γ is increased, the circulation and physical size of the eddy increases [3]. During this process, the forward stagnation point moves upstream slightly, while the rearward stagnation point moves downstream rapidly.

Some remarks about the base flow are in order at this point. They take the form of three qualifications.

a. The base flow assumes axisymmetry. The flow is intended to simulate the phenomenon of vortex breakdown, but recent experimental work has shown that this phenomenon displays a number of non-axisymmetric features [4]. One form of breakdown is, however, referred to as axisymmetric and its bubble-like forebody is similar in appearance to the forebody of the eddy shown in Fig. 3(a). It now appears that the axisymmetric form is observed only at very high Reynolds numbers ($Re > 500$). Its downstream wake is not axisymmetric and does not appear to contain a stagnation point. The wake also provides a mechanism for bulk exchange of fluid between the eddy and the support stream. It is not yet possible to numerically simulate such a three dimensional flow field and the base flow is perhaps the best that can be done at present.

b. All of the present results pertain to parameter values of $Re = 50$, $\Gamma = 1$ and $B = 8$. As noted above, computed axisymmetric flows vary with these parameters in a complex way. Since the present results do not vary the base flow systematically they must in that sense be viewed as preliminary.

c. An inviscid, rotating stream is known to be dispersive to waves [5]. The effect of viscosity or the imposed boundary conditions on damping out such dispersion is not known. Thus, some aspects of the flowfield boundary conditions may actually serve to keep the breakdown stationary.

DIFFUSION

Confinement will be examined by watching the inter-diffusion of two molecular species, A and B. We will denote the fluid we wish to contain or supply by A, and the support stream by B. The governing nondimensional equation for transport of species A, expressed as a mass fraction Y of the total mixture, is

$$\frac{\partial Y}{\partial t} + \frac{\partial(uY)}{\partial x} + \frac{1}{r} \frac{\partial(rvY)}{\partial r} = \frac{1}{ReSc} \cdot \left\{ \frac{\partial^2 Y}{\partial x^2} + \frac{1}{r} \frac{\partial}{\partial r} \left(r \frac{\partial Y}{\partial r} \right) \right\} \quad (1)$$

assuming an equi-molar, constant property process. Equation (1) introduces the Schmidt number, $Sc = \nu/D$, as a parameter where D is the mass diffusion coefficient. Time is scaled with r_o/U . The molecular weights of A and B are presumed equal in order to maintain density constant. With constant density, incompressible flow fields determined previously may be used as base flows into which diffusion may be introduced. The velocity or streamline field is uncoupled from the diffusion problem and does not change as the process of equi-molar, equi-mass diffusion takes place.

For Problem I the entire inlet flow is species B($Y=0$). In Problem II a

stream of species A of radius r_A is bled in along the axis ($Y=1$ for $r \leq r_A$). The axial velocity at the inlet is uniform. In both problems no mass flow crosses the tube wall or tube centerline ($\partial Y / \partial r = 0$), and no axial diffusion is presumed to occur at the exit ($\partial Y / \partial x = 0$). The latter is a weak boundary condition consistent with boundary layer behavior.

Initial data consists of filling the eddy with species A($Y=1$) for Problem I while the remaining region is species B($Y=0$). For Problem II the entire initial field was taken to be species B($Y=0$).

NUMERICAL SOLUTION

With the aforementioned boundary conditions finite-difference solutions to Eq. (1) have been obtained by the method described in [3]. The velocity field is constant with time and was the previously obtained solution for $Re = 50$, $\Gamma = 1$, and $B = 8$ which has already been discussed. The field of mass fraction Y is explicitly advanced in time from the initial state to a steady state. Finite difference approximations of Eq. (1) are applied to all interior grid points, to the axis, and to the tube wall. Conditions at the inlet were held constant. An extra column of mesh points with field values equated to those at the last computed column was added at the exit to satisfy the downstream boundary condition.

Concentration fields are printed out at various points in the transient (which was always a smooth transition), together with various mass diffusion rates. The transient for Problem I is complete when the initial contents of the eddy completely diffuse into the support stream. For Problem II, the transient is complete when a steady concentration field is established.

Mesh increments of $\Delta x = 0.125$ and $\Delta r = 0.05$ (41 x 21 grid) were employed. This is a rather fine mesh but was necessary in order to faithfully describe the boundary of the eddy and the transport processes there.

RESULTS

The present diffusion calculations are, by themselves, believed to be quite reliable and thus can shed some light on diffusional processes in a flow field. The calculations are performed for $Re = 50$ but may be thought of as simulating an isotropic turbulent field with the molecular viscosity in the Reynolds number replaced by a turbulent eddy viscosity. As mentioned earlier, the base flow itself should be viewed with care and thus regarded only as a test case.

Problem I - Depletion

It is useful to regard this part of the study as a test of the effectiveness of fluid containment in a given internal stagnation region. We assume that a contained mass could be established and then follow the decay process as species A diffuses out of the region and is replaced by species B.

Figure 1 illustrates the decay of species A as a function of time for $Sc = 0.1, 1, 10$, and infinity. The ordinate is the normalized mass of A in the eddy. The rate of decay decreases with larger values of Sc , thus leading to more effective containment. Schmidt numbers near 1 are associated with ordinary gases, and larger values up to about 10 are associated with liquids. A unit of dimensionless time is equal to Ut'/r_0 and represents the time required for the mass flow to traverse a distance of one radius. Thus, depletion is seen to be rapid in all cases of interest. The fluid residence time is of course, expected to depend on Re and Γ , and on the density difference between species A and B. The assumption of constant density must be relaxed to examine a wider range of containment problems.

The nondimensional initial mass is equal to 0.392. This is also the volume of the eddy as approximated in the Eulerian computing grid. In such a grid there is a convective and diffusive mass flux between grid points and across the boundary of the eddy. In theory, only a diffusive mass flux across the eddy boundary exists. The exact treatment of this flux would necessitate a Lagrangian grid in which grid lines follow streamlines (the eddy boundary $\psi = 0$ would then be a grid line). The present numerical scheme can only approximate the requirement of no convection across streamlines. In order to assess the effect of such transport velocities, calculations were undertaken with the transport velocities across the Eulerian representation of the eddy boundary set equal to zero. Results are shown as dashed lines in Fig. 1. The solid lines represent results from the unmodified Eulerian calculation. For $Sc = 0.1$ and 1.0 , the dashed lines and solid lines coincide, that is, the contribution of convective transport across the boundary to the depletion of species A is negligible. However, around $Sc = 10$, it appears that depletion is predominantly by diffusion, but that convection is becoming significant. The solid line for $Sc = \infty$ coincides with the dashed line for $Sc = 10$ and is not shown. The large difference between the solid and dashed lines for $Sc = \infty$ indicates that the Eulerian grid representation is inappropriate, and suggests that the range of physical validity of the results is restricted to $Sc < 10$.

Certain aspects of the concentration field during the mass diffusion transient are illustrated in Fig. 2. The three columns from left to right correspond to $Sc = 10, 1$, and 0.1 , in order of increasing mass diffusivity. The solid line designates the 5 percent concentration line for species A ($Y = 0.05$), the dashed line the eddy shape, and the small dot the point of maximum concentration. For $Sc = 10$, the axial convection of species A away from the eddy is relatively stronger than the radial diffusion. The shape of the 5 percent concentration line becomes elongated, and an annular wake develops downstream. That is, the concentration profile does not achieve a maximum on the axis, but intermediate to the axis and wall. For $Sc = 1$, mass diffusion is enhanced relative to axial convection. For $Sc = 0.1$ the process of mass diffusion away from the eddy is more significant than axial convection, and an annular wake never develops. Early in the transient for all Schmidt numbers the 5 percent concentration line remains congruent with the eddy shape. This follows because the maximum concentration gradient for species A is in a direction normal to the boundary of the eddy.

Problem II - Filling

The replenishment of fluid to the eddy might be accomplished by any of several injection mechanisms. Here, injection using a jet on the axis at the inlet is considered. By examining steady state concentration contours the size of regions maintained at high concentrations can be determined.

Concentration fields are shown in Figs. 3(b) to 3(e) for various inlet radii r_A ranging from 0.025 to 0.425. A unit Schmidt number is assumed. Each solid line corresponds to a particular value of mass fraction Y as indicated. The dashed line is the eddy boundary. A region of high concentration is found only near the forward stagnation point and is distorted and generally follows the pattern of fluid flow around the eddy. A large region of nearly uniform concentration is found near the downstream portion of the eddy (approximately $x = 0.5$ to 1.7) and in the downstream wake ($x = 1.7$ to 4.5). Migration of a given concentration line (such as $Y = 0.1$) downstream with increasing r_A illustrates the dependence of the concentration field on the radius of the inlet stream.

Diffusion is a significant transport process at unit Schmidt number (the product $ReSc$ in the species transport equation, Eq. (1), is equal to fifty) and the inlet stream of species A tends to diffuse rapidly into the support stream of species B. This, coupled with the large surface area of the eddy relative to that of the inlet stream, makes effective containment within the eddy difficult. Rapid diffusion out of the eddy was also apparent in the results of the previous section.

The region of high concentration near the forward stagnation point, on the other hand, suggests the possibility of using that region for fluid containment. The reduced velocities and the pattern of flow near the stagnation zone lead to effective confinement. Further support for the use of this region for containment follows from the relative insensitivity of the location of the forward stagnation point to changes in Re or Γ , at least for the conditions specified for the base flow [3]. Although there is a steady flow through the stagnation point region, that region still represents an internally-confined fluid zone of high concentration.

The effectiveness of fluid confinement by a flow with an internal stagnation point, as compared to one without, was assessed by undertaking a series of calculations on jet diffusion. A uniform axial flow with no rotation was employed ($u = 1$, $v = 0$, $w = 0$ throughout the tube). The core of the inlet stream, radius $r \leq r_A$, consisted of fluid A. There is no internal stagnation zone and no shear associated with such a jet, and mixing is completely controlled by molecular diffusion.

Concentration contours for jets with $r_A = 0.025$ and 0.425 are shown as dotted lines in Figs. 3(b) and 3(e), respectively. For inlet streams larger than about $r_A = 0.025$ results are similar to those shown in Fig. 3(e). Under such conditions the flow with a stagnation point has a much larger region of high concentration of species A than does the jet flow. In Fig. 3(e), the volumes enclosed by the $Y = 0.5$ and 0.2 concentration lines are about twice as large with stagnation as compared with a pure jet. For inlet streams of about $r_A = 0.025$ or smaller the reverse is true. The latter is attributed to the

enhancement of diffusive mixing by the eddy, as the inlet stream of A forms an annular jet with correspondingly greater surface area. For sufficiently large r_A , on the other hand, a flow with a stagnation zone is more effective for fluid confinement than is the jet flow.

The use of an interior stagnation region to achieve fluid confinement requires some estimate of the flow rate through, and mass contained in, a particular volume of space. For the present, it is convenient to consider the volume occupied by the eddy. The mass of species A inside the eddy relative to the total mass of the eddy is illustrated in Fig. 4 (left hand ordinate) as a function of the radius of the inlet stream, r_A . As r_A increases the mass of species A inside the eddy increases, yielding an s-shaped curve which approaches unity as $r_A \rightarrow 1$ (eddy filled 100%). For small values of r_A (less than 0.3), the contained mass of species A varies as r_A^2 . In other words, it varies in direct proportion to the mass flow rate of A at the inlet.

The effectiveness of fluid capture can also be assessed by examining the rate of diffusion of species A into (or out of) the eddy relative to the flow rate of species A at the inlet. This is shown in Fig. 4 (right hand ordinate). The efficiency of capture rises from about 32% to a maximum of 34% as r_A increases from near zero to 0.225. As r_A increases from 0.225 to 1.0, the efficiency decreases to about 5%. Species A originating at large radii in the inlet tends to flow around the eddy rather than diffusing into it. Clearly, inlet radii less than about 0.3 are suggested if the eddy is to be used efficiently for containment.

CONCLUSIONS

This preliminary study allows two conclusions to be drawn:

- a. The fluid holding time within a recirculation zone is of the order of several time units at best. (A time unit is r_0/U .) The effects of Re , Γ , and large density differences between contained and support flow on the decay transient remain to be assessed.
- b. An internal stagnation point, if it can be maintained, appears to offer the best potential for fluid self-confinement. The confinement is relative, of course, and requires a more complete assessment of the effects of Re , Γ , and Sc .

REFERENCES

1. R.G. Ragsdale, "Status of Open-Cycle Gas-Core Reactor Project through 1970," NASA TM X-2259, NASA, Washington, D.C., 22p., March 1971.
2. F.K. Moore and S. Leibovich, "Self-confined Rotating Flows for Containment," Proceedings of the NASA Symposium on Research on Uranium Plasmas and Their Technological Applications, p. 95, NASA SP-236, NASA, Washington, D.C., 1971.
3. K.E. Torrance and R.M. Kopecky, "Numerical Study of Axisymmetric Vortex Breakdowns," NASA CR-1865, NASA, Washington, D.C., 37p., August 1971.
4. T. Sarpkaya, "Vortex Breakdown in Swirling Conical Flows," A.I.A.A. Journal, 9, p. 1792, 1971.
5. T.B. Benjamin, "Upstream Influence," J. Fluid Mech., 40, p. 49, 1970.

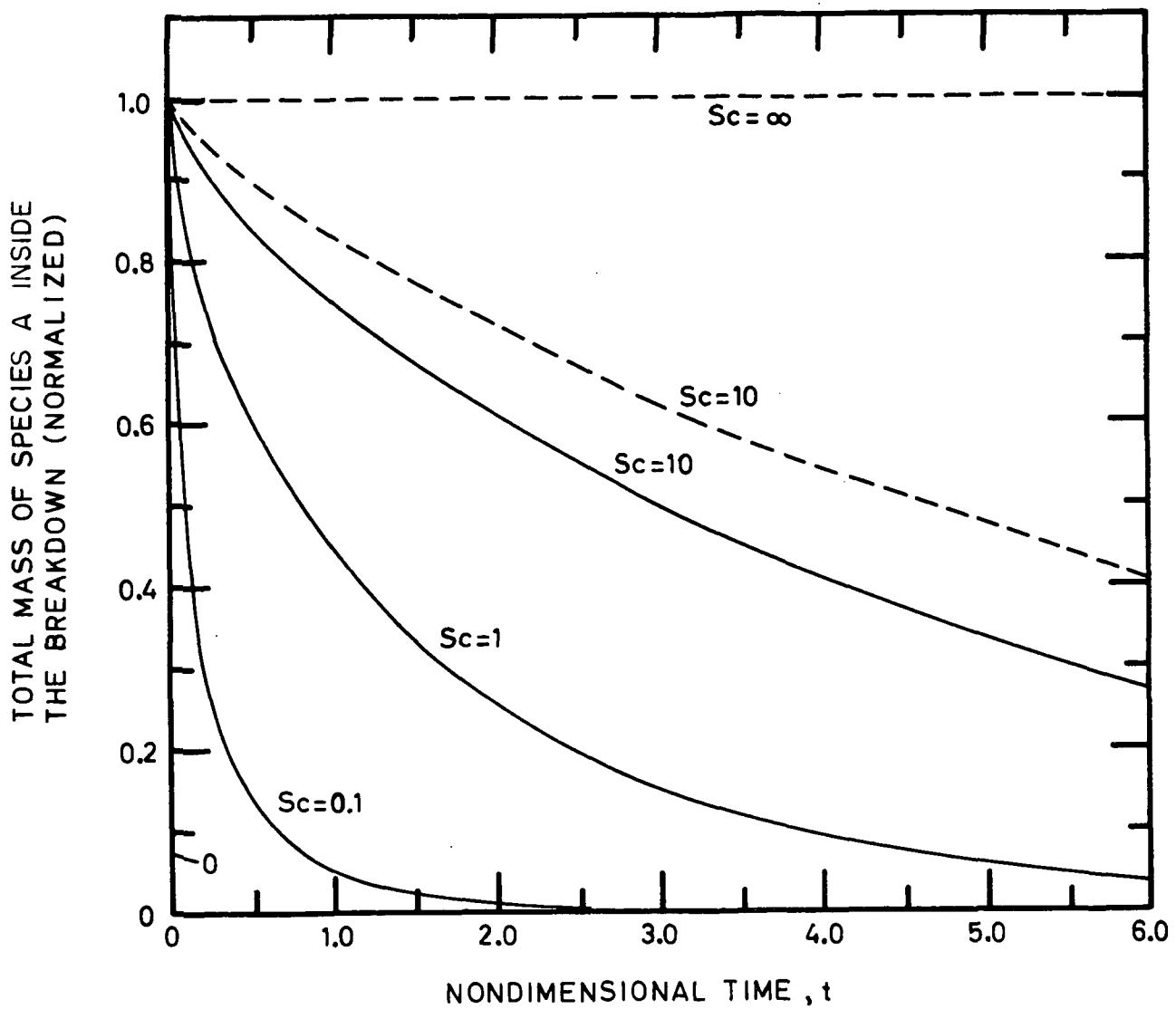


Fig. 1. Decay transient for various Schmidt numbers (Sc). Eddy filled with species A at $t = 0$. For $t > 0$, diffusion occurs depleting the mass of species A in the eddy. Dashed line indicates the effect of setting transport velocities in the Eulerian grid equal to zero across the eddy boundary. This and all subsequent figures apply for $Re = 50$, $\Gamma = 1$, and $B = 8$.

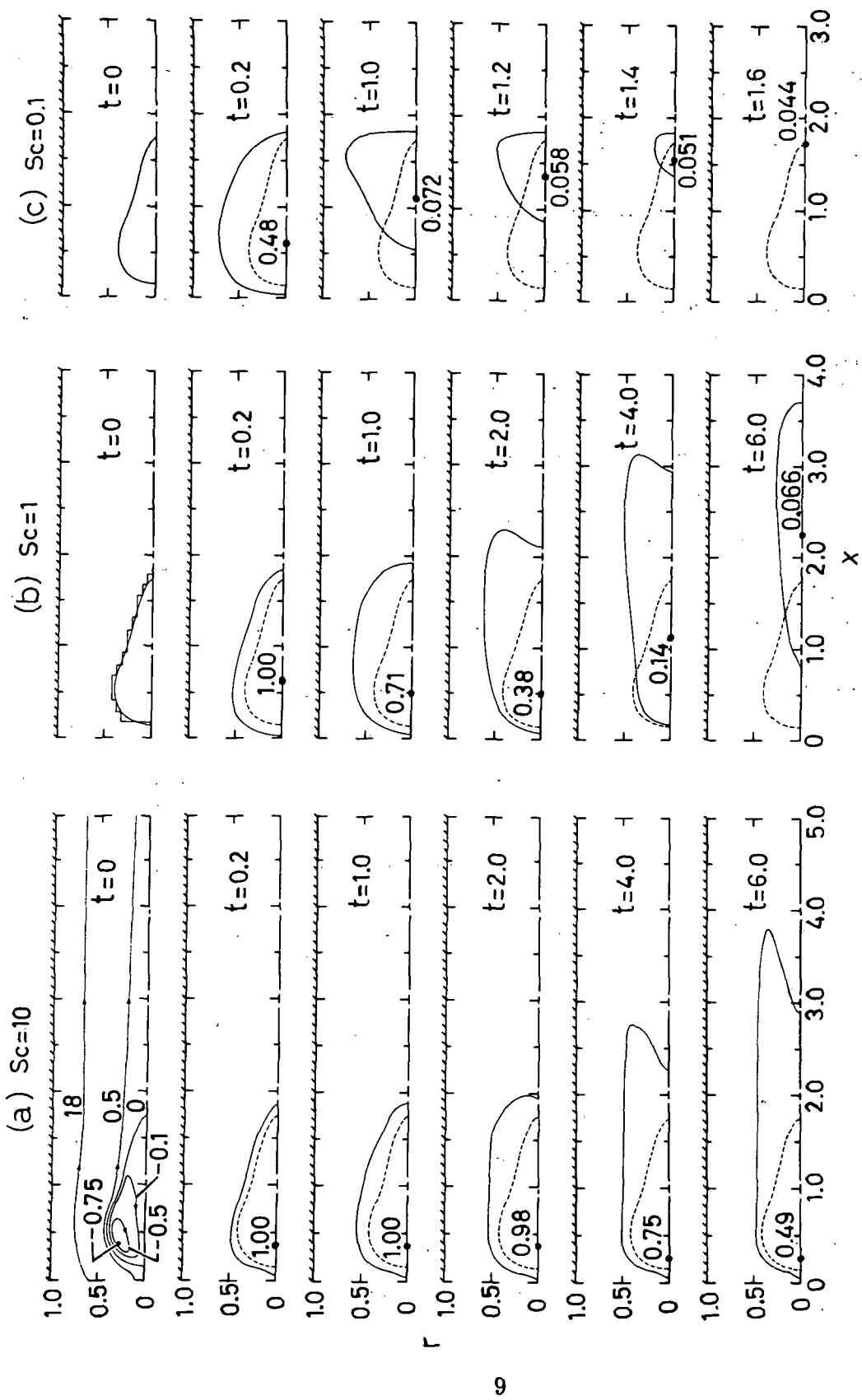


Fig. 2. Concentration fields associated with the decay transient of Fig. 1. The solid line denotes the $Y = 0.05$ contour; the small dot locates the point of maximum concentration, the value of which is stated. The dashed line for $t > 0$ is the boundary of the eddy. Streamlines are shown in the graph at the upper left (stream function values equal those shown $\times 10^{-2}$).

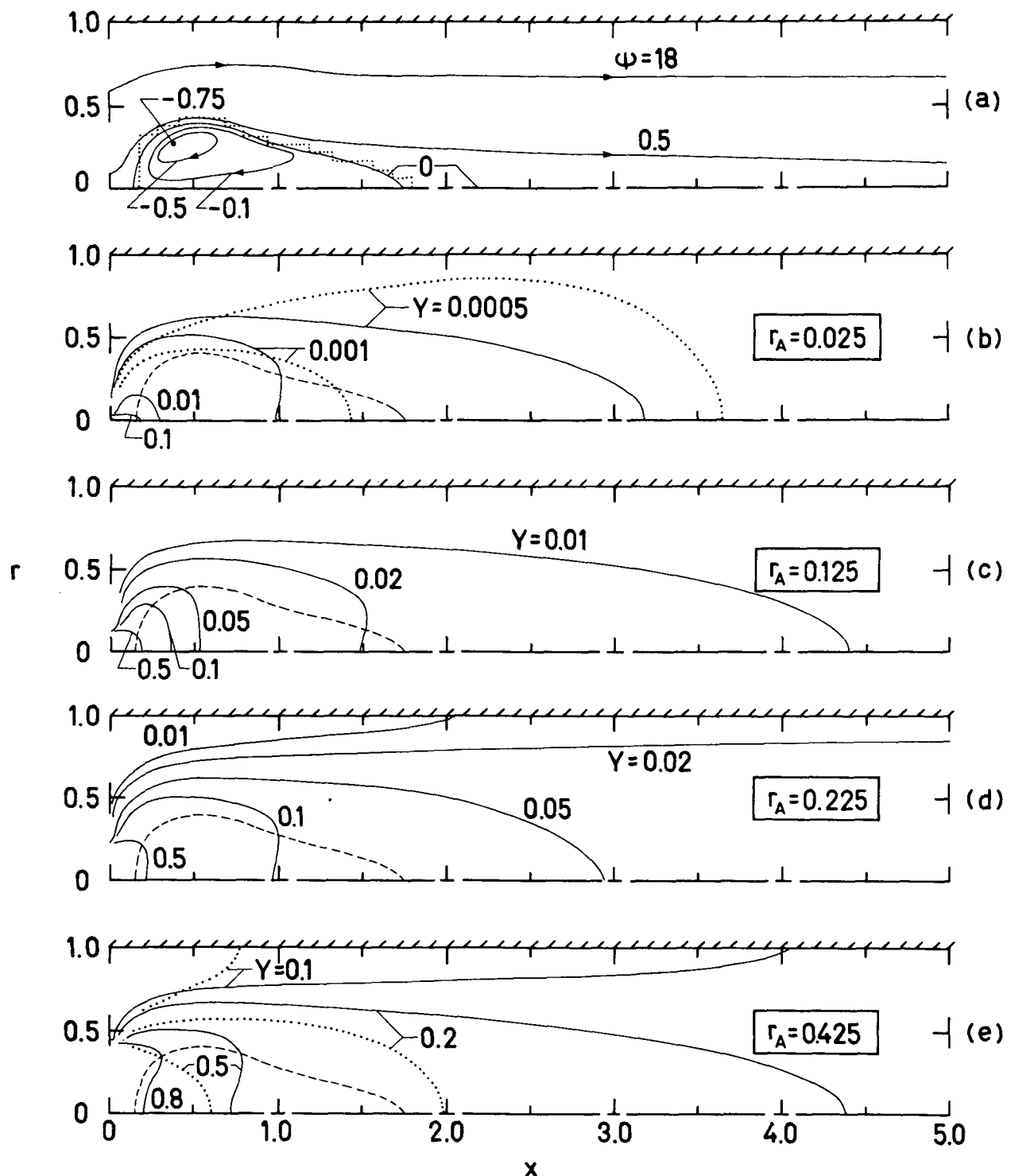


Fig. 3. Steady state concentration fields, $Sc = 1$. (a) Base flow streamlines (stream function values equal those shown $\times 10^{-2}$). (b) to (e) Concentration lines for supply streams of various radii r_A . Dotted lines are for jet diffusion.

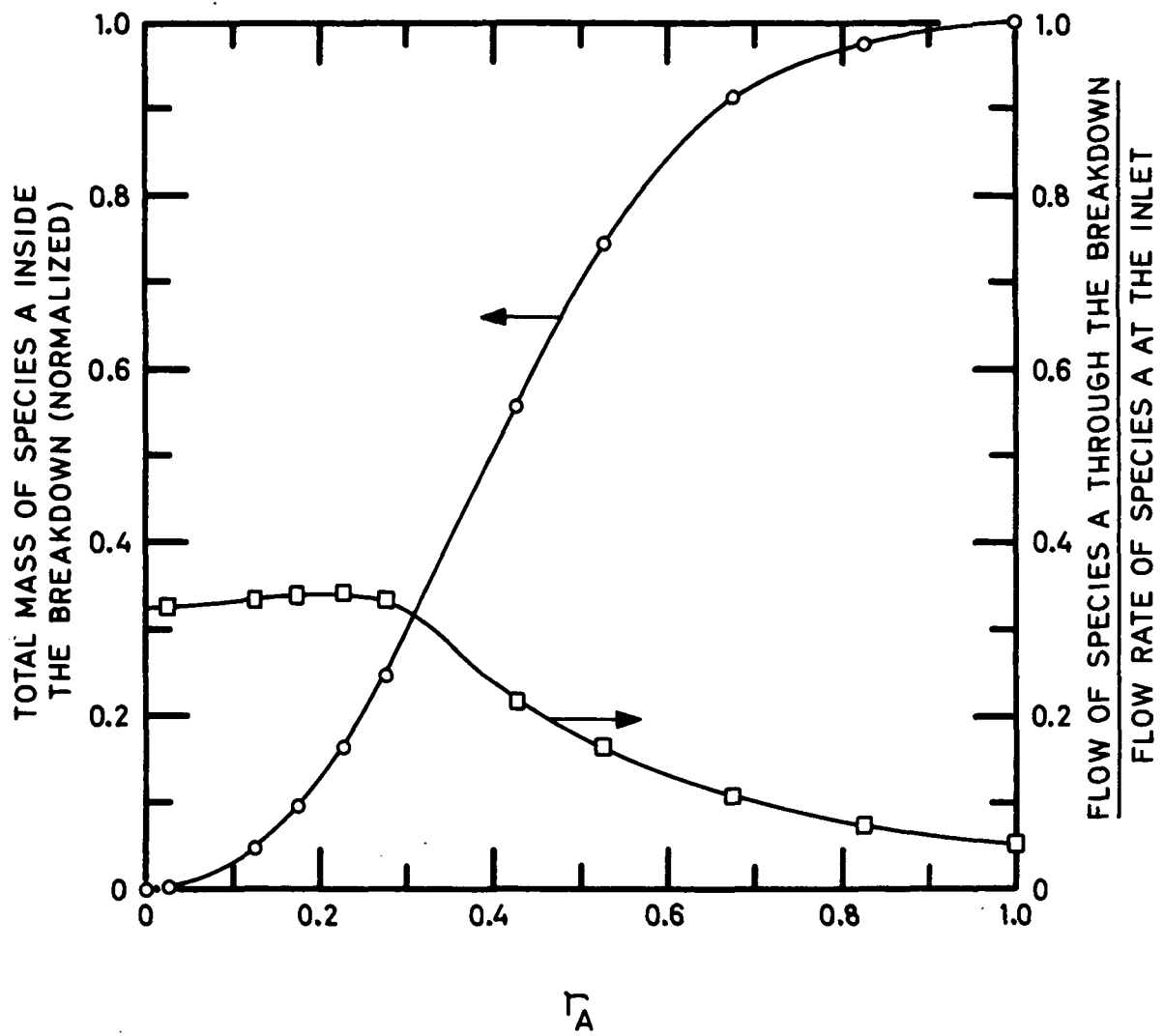


Fig. 4. Mass of species A contained in an eddy and mass flow of species A through an eddy at steady state using supply streams of various radii, r_A . $Sc = 1$.

NATIONAL AERONAUTICS AND SPACE ADMINISTRATION
WASHINGTON, D.C. 20546

OFFICIAL BUSINESS
PENALTY FOR PRIVATE USE \$500

SPECIAL FOURTH-CLASS RATE
BOOK

POSTAGE AND FEES PAID
NATIONAL AERONAUTICS AND
SPACE ADMINISTRATION
451



POSTMASTER

If Undeliverable (Section 108
Postal Manual) Do Not Return

"The aeronautical and space activities of the United States shall be conducted so as to contribute . . . to the expansion of human knowledge of phenomena in the atmosphere and space. The Administration shall provide for the widest practicable and appropriate dissemination of information concerning its activities and the results thereof."

—NATIONAL AERONAUTICS AND SPACE ACT OF 1958

NASA SCIENTIFIC AND TECHNICAL PUBLICATIONS

TECHNICAL REPORTS. Scientific and technical information considered important, complete, and a lasting contribution to existing knowledge.

TECHNICAL NOTES. Information less broad in scope but nevertheless of importance as a contribution to existing knowledge.

TECHNICAL MEMORANDUMS. Information receiving limited distribution because of preliminary data, security classification, or other reasons. Also includes conference proceedings with either limited or unlimited distribution.

CONTRACTOR REPORTS. Scientific and technical information generated under a NASA contract or grant and considered an important contribution to existing knowledge.

TECHNICAL TRANSLATIONS. Information published in a foreign language considered to merit NASA distribution in English.

SPECIAL PUBLICATIONS. Information derived from or of value to NASA activities. Publications include final reports of major projects, monographs, data compilations, handbooks, sourcebooks, and special bibliographies.

TECHNOLOGY UTILIZATION PUBLICATIONS. Information on technology used by NASA that may be of particular interest in commercial and other non-aerospace applications. Publications include Tech Briefs, Technology Utilization Reports and Technology Surveys.

Details on the availability of these publications may be obtained from:

SCIENTIFIC AND TECHNICAL INFORMATION OFFICE

NATIONAL AERONAUTICS AND SPACE ADMINISTRATION

Washington, D.C. 20546